Geometric scaling and multiplicity distribution in high-energy pp collisions*

R. Torgerson and A. N. Kamal

Theoretical Physics Institute, Department of Physics, University of Alberta, Edmonton, Alberta, Canada

(Received 12 May 1975)

We find an empirical representation, employing geometric scaling, for the profile function at CERN ISR energies (23.5 GeV $\leq \sqrt{s} \leq$ 53 GeV). A Fermi distribution dominates the profile function shape but a small negative Gaussian term is required to fit $d\sigma/dt$ in the region of the secondary maximum. We find a sharp peak in the opacity at $b = 0$. These results are used to discuss a variety of geometric proposals for understanding the multiplicity distribution.

I. INTRODUCTION

Geometric intuitions have been a constant source of inspiration concerning the collisions of strongly interacting particles since the introduction of the optical model into nuclear physics 26 years ago.[1] The concept of interpenetrating absorptive droplets with hadronic matter distributed in the same way as the measured charge distribution of the proton was an important development in such geometric notions.[2] Although this model fits[3,4] the pp elastic differential cross section at CERN ISR energies for small t, it fails to represent the data in shape and energy dependence in the region of the secondary peak[4,5]; see also the dashed line of Fig. 1. A different geometric idea, namely, scaling in impact-parameter space,[6,7] seems to be suggested by the energy dependence of the secondary peak. In this concept the hadron-hadron opacity is thought to be expanding in a shape-independent way. If Ω (b, s) is the opacity then

$$\Omega(b, s) = \bar{\Omega}\,(b/R(s)), \tag{1}$$

where $R(s)$ is the effective overlap radius of the hadrons and b the impact parameter. Since for purely real $\Omega(b, s)$,

$$\begin{aligned}\sigma_T &= 4\pi \int b\, db(1 - e^{-\Omega(b,s)}) \\ &= 4\pi R^2(s) \int x\, dx(1 - e^{-\bar{\Omega}(x)}),\end{aligned} \tag{2}$$

$\sqrt{\sigma_T}$ is a suitable alternative to $R(s)$. This idea, geometrical scaling, evolved from attempts to understand Koba-Nielsen-Olesen (KNO) scaling[8] in a geometric way.[6,7,9-13] It may indeed be a very fundamental concept since it was derived[14] some time ago from axiomatic field theory under the assumption that $\sigma_T \sim \ln^2 s$.

II. THE PROFILE FUNCTION

We parameterize the profile function Γ by use of a Fermi function and a Gaussian:

$$\begin{aligned}\Gamma &= 1 - e^{-\Omega} \\ &= N_0 \left(\frac{1}{1 + e^{(b - B_0)A}} + \frac{C}{2} e^{-b^2/4D} \right),\end{aligned} \tag{3}$$

and fit to the experimental differential cross section via

$$\frac{d\sigma}{dt} = \pi \left| \int_0^\infty b\, db J_0(b\sqrt{-t}\,)\Gamma(b) \right|^2, \tag{4}$$

where t is the invariant momentum transfer and A, B_0, C, D, N_0, are the parameters. The differential cross section can be fitted very well by the Fermi term alone for small t but fails in the region of the secondary maximum. The addition of a small Gaussian correction enables one to fit the large-t region as well. By trial and error we found that the parameter set A, B_0, C, and D listed in row 1 of Table I yields a good fit to the relative differential cross section[15] for $\sqrt{s} = 53$ GeV and -5.2 (GeV$/c)^2 \leq t \leq 0$; see Fig. 1. The parameter N_0 is determined afterwards by the experimental value[16,17] of σ_T at $\sqrt{s} = 53$ GeV. Geometric scaling implies

$$\begin{aligned} &A \propto R(s)^{-1}, \\ &B_0 \propto R(s), \\ &C \propto \text{constant} \\ &D \propto R(s)^2, \\ &N_0 \propto \text{constant}. \end{aligned} \tag{5}$$

Consequently, the total cross section may be used to determine $d\sigma/dt$ at $\sqrt{s} = 44.9$, 30.7, and 23.5 GeV. As seen in Fig. 1, the prediction is in reasonable over-all agreement with experiment.[15] We now express Γ as a function of the scaled variable $x = b/R(s)$. For $R(s)$ we take the rms separation between the two extended protons:

$$R(s)^2 = \frac{\int_0^\infty \Omega(b, s) b^3\, db}{\int_0^\infty \Omega(b, s) b\, db}\,. \tag{6}$$

At $\sqrt{s} = 53$ GeV, $R(s) = 4.88$ (GeV$/c)^{-1} = 0.963$ fm.

Thus we find from Eq. (3) and Table I

$$\bar{\Gamma}(x) = 0.92\left(\frac{1}{1+e^{2.87(x-0.666)}} - 0.055e^{-15.3x^2}\right). \tag{7}$$

In Fig. 2 we plot the opacity as a function of the scaling variable x. In the inset of Fig. 2 we compare our opacity with that of Ref. 4 for $\sqrt{s} = 53$ GeV. The only significant disagreement apparent on a linear plot is in the region $0 < x \lesssim 0.4$, showing that the opacity should be more peaked near the origin than often realized.[18]

The Fermi function dominates the differential cross section for large b and therefore small t. It has the characteristic feature that the slope parameter $B = (d/dt)\ln(d\sigma/dt)$ increases gradually as $t \to 0$, as the data require. This illustrated in Table II where the t variation in the slope parameter is studied and related to the available data.[17,19] Although we have kept the Gaussian term for this comparison, setting it equal to zero makes no significant difference.

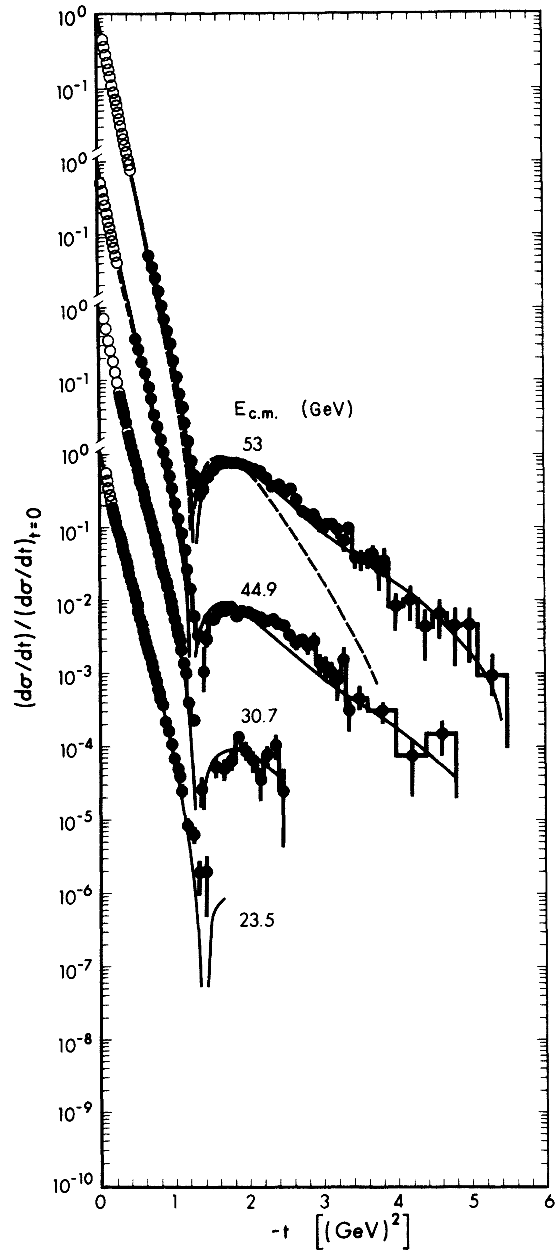

FIG. 1. The proton-proton relative differential cross section $(d\sigma/dt)/(d\sigma/dt)_{t=0}$ at $\sqrt{s} = 53$, 44.9, 30.7, and 23.5 GeV compared to our model indicated by a solid curve. The dashed curve corresponds to the model of Ref. 4.

III. THE MULTIPLICITY DISTRIBUTION

There have been many proposals for relating information on elastic scattering at impact parameter b to particle production. Perhaps the simplest is the assumption that the multiplicity distribution for impact parameter b has zero width.[6,9,12,13] In this paper we use this ansatz together with the impact-parameter profile function determined above to find $n(b, s)$, the number of particles produced at impact parameter b from the known multiplicity data.

We follow the method of Ref. 20. Let

$$O(b, s) = 1 - e^{-2\Omega}$$
$$= \Gamma(2 - \Gamma) \tag{8}$$

be the overlap function. The cross section for producing n charged particles is given by

$$\sigma_n = 4\pi \int_0^\infty b\, db O(b, s)\delta(n - n(b, s)). \tag{9}$$

This implies that the average multiplicity is given by

$$\langle n \rangle = \frac{\int_0^\infty b\, db O(b, s) n(b, s)}{\int_0^\infty b\, db O(b, s)}. \tag{10}$$

Since the high-energy behavior of $R(s)$ is consistent with $\ln s$ we can provide for the energy dependence of the average multiplicity $\langle n \rangle$ by the ansatz

$$n(b, s) = KRf(b/R) = KRf(x), \tag{11}$$

where K is chosen to satisfy $KR = \langle n \rangle$. The KNO scaling function ψ becomes

$$\psi = \langle n \rangle \frac{\sigma_n}{\sigma_{\text{inel}}}$$
$$= \frac{\pm 2b_n O(b_n, s) db_n/df}{\int_0^\infty b\, db O(b, s)}. \tag{12}$$

TABLE I. Determination of parameters.

$\sqrt{s}$ (GeV)	σ_T [a] (mb)	A (GeV/c)	B_0 [(GeV/c)$^{-1}$]	C	D [(GeV/c)$^{-2}$]	N_0
53.0	43.1 ± 0.5	0.589	3.25	−0.110	0.388	0.920
44.9	42.5 ± 0.4	0.593	3.23	−0.110	0.383	0.920
30.7	40.6 ± 0.4	0.606	3.15	−0.110	0.365	0.920
23.5	39.1 ± 0.4	0.618	3.10	−0.110	0.352	0.920

[a] Combined data of Ref. 16 and Ref. 17

The + (−) sign results from assuming that f is an increasing (decreasing) function of b. The impact parameter b_n is determined by solving

$$\frac{n}{\langle n\rangle} = f(b/R(s)) \qquad (13)$$

for b. Equations (12) and (13) and geometric scaling, $O(b, s) = \tilde{O}(b/R(s))$, imply[6] that ψ is a function of the reduced multiplicity $z \equiv n/\langle n\rangle$ only, i.e., KNO scaling. For $\psi(z)$ we adapt a simple, fairly accurate representation of the pp multiplicity data given some time ago[9]

$$\psi(z) = \pi z\, e^{-(\pi/4)z^2}\,. \qquad (14)$$

Using Eqs. (12)–(14) one can integrate both sides and obtain

$$e^{-(\pi/4)z^2} = \frac{\int_{f_+^{-1}(z)}^{\infty} x\, dx\, \tilde{O}(x)}{\int_0^{\infty} x\, dx\, \tilde{O}(x)}\,, \qquad (15)$$

$$e^{-(\pi/4)z^2} = \frac{\int_0^{f_-^{-1}(z)} x\, dx\, \tilde{O}(x)}{\int_0^{\infty} x\, dx\, \tilde{O}(x)}\,. \qquad (16)$$

The function $f_+^{-1}(z)$ $[f_-^{-1}(z)]$ is the function inverse to $f(x)$ in case $f(x)$ is an increasing (decreasing) function of x. We have determined $f_\pm(x)$ from Eqs. (15) and (16) by numerical integration using our results for $\tilde{\Gamma}$. For convenience we have found simple analytic formulas to represent the results approximately:

$$f_+(x) = 1.018x^{0.85}, \qquad (17)$$

$$f_-(x) = 2.78e^{-1.2x}\,. \qquad (18)$$

In Table III, we compare the reduced moments

$$C_q = \langle n^q\rangle / \langle n\rangle^q$$

determined from Eqs. (12), (17), and (18) with those derived from experiment.[21] In column 5 of Table III we have also listed the reduced moments derived directly from Eq. (14). The degree of discrepancy between columns 2 and 5 or 3 and 5 reflects the fact that the simple analytic representations give the main trends for the functional behavior of the $f_\pm(x)$ derived by numerical integration but not the detailed shape. We doubt that the detailed shape has any significance at the present time since the C_q values, especially the ones for larger q, may show some modest increase at higher energy.[22]

Our results for $f_\pm(x)$ are qualitatively very similar but not identical to the graphical results presented in Ref. 20. Equation (17) is similar also to the proposal of Ref. 12, namely

$$z = x. \qquad (19)$$

The discrepancy between Eqs. (17) and (19) is quantitatively significant, since (19) predicts C_q values that are much too large for large q. For example, C_6 is twice the experimental value.

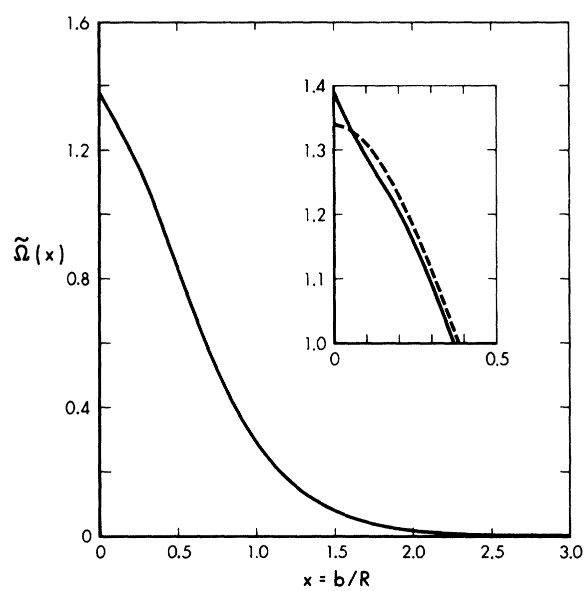

FIG. 2. The opacity derived from our fit to the differential cross section for pp scattering plotted as a function of $x = b/R$. In the inset our opacity (solid curve) is compared with that of Ref. 4 (dashed curve) for $\sqrt{s} = 53$ GeV.

TABLE II. Variation of the slope parameter, $B = \Delta \ln(d/dt)/\Delta t$.

$\sqrt{s}$ (GeV)	t interval [(GeV/c)^2]	B experiment [(GeV/c)$^{-2}$]	B theory [(GeV/c)$^{-2}$]	t interval [(GeV/c)^2]	B experiment [(GeV/c)$^{-2}$]	B theory [(GeV/c)$^{-2}$]	$B(t=0)$ theory [(GeV/c)$^{-2}$]
53.0	−0.308, −0.168	10.8 ± 0.2 [a]	11.0	−0.06, −0.01	13.1 ± 0.3 [b]	13.2	13.9
44.9	−0.239, −0.136	10.8 ± 0.2 [a]	11.2	−0.05, −0.01	12.6 ± 0.4 [b]	13.1	13.7
30.7	−0.240, −0.138	10.9 ± 0.2 [a]	10.8	−0.090, −0.046	11.9 ± 0.3 [a]	12.0	13.1
23.5	−0.238, −0.138	10.4 ± 0.2 [a]	10.4	−0.094, −0.050	11.6 ± 0.3 [a]	11.5	12.6

[a] Reference 19
[b] Reference 17

This disagreement is due to the extended character of our solution for $\tilde{\Gamma}(x)$.

An "up" solution such as Eq. (17) or (19) is difficult to understand from the geometric point of view since one readily imagines that there will be more hadrons produced in central collision than in peripheral ones. Thus, "down" solutions are very popular. One such example is $n(b, s) \propto \Omega(b, s)$ which is believed[20,23] not to be realistic. This is clear in the context of the zero width ansatz since $\tilde{\Omega}(x)$ is very poorly approximated by the $f_-(x)$ of Eq. (18). A more realistic example is the proposal[13]

$$n(b, s) \propto \Gamma(b, s). \tag{20}$$

We have listed the results of Ref. 13 in column 6 of Table III. They are in reasonable agreement with experiment. This work assumed the usual Gaussian for the profile function. However, when our more extended Γ is applied to the ansatz of Eq. (20) then the agreement with experiment deteriorates. (See column 7 of Table III.) This deterioration is to be expected since the functional form of $\tilde{\Gamma}(x)$ given in Eq. (7) is very poorly approximated by $f_-(x)$ of Eq. (18).

Another simple proposal for the multiplicity distribution at impact parameter b is based on eikonal-type ideas. Here the cross section for having N open chains or towers is[10,11,24,25]

$$\sigma(N) = \int d^2b\, e^{-2\Omega} \frac{(2\Omega)^N}{N!}. \tag{21}$$

It is easy to show that geometric scaling implies that $\langle N \rangle$ is energy independent. As in the previous approach one may accommodate the energy dependence of $\langle n \rangle$ by requiring that n_1, the number of particles produced per chain, grows as $R(s)$. For simplicity we follow Ref. 10 in assuming that the number distribution of particles produced per chain has a zero width. In terms of the reduced moments C_q we find

$$C_q = \frac{\int_0^\infty b\, db \sum_{m=0}^{\infty} \mathcal{S}_q^{(m)} (2\Omega)^m \left(\int_0^\infty b\, db O\right)^{q-1}}{\left(\int_0^\infty b\, db (2\Omega)\right)^q}, \tag{22}$$

where the $\mathcal{S}_q^{(m)}$ are Stirling numbers of the second kind.[26] Using geometric scaling in Eq. (22) one easily finds that the C_q are s-independent. With a step function for Γ one observes[10] that the first few C_q are in crude agreement with experiment. However when one inserts our Ω in Eq. (22) the results are very poor; for example, C_5 is three times the experimental value.

IV. SUMMARY

We started with a Fermi-function form for the profile function with three parameters. It was generally possible with this simple form to fit

TABLE III. Comparison of reduced moments C_q with experiment.

q	Theory (+ case) Eq. (17)	Theory (−case) Eq. (18)	Experiment Ref. 21	Eq. (14)	Theory Ref. 13	Theory Eq. (20)
2	1.22	1.30	1.24 ± 0.006	1.27	1.37	1.46
3	1.74	1.99	1.81 ± 0.02	1.91	2.14	2.44
4	2.83	3.42	2.97 ± 0.06	3.24	3.56	4.41
5	5.16	6.39	5.36 ± 0.15	6.08	6.2	8.34
6	10.4	12.7	10.43 ± 0.39	12.4	11.2	16.3
7	23.2	26.2	21.6 ± 1.1	27.1	20.6	32.4
8	56.5	56.4	47.0 ± 2.8	63.1	39	65.7

the forward peak, the dip; and much of the secondary peak. The calculated differential cross section, however, tended to drop for large t's faster than the data. To shift the zero of the amplitude to higher t values we added a short-range Gaussian with two extra parameters which corrected the large-t behavior and at the same time had little effect on the forward peak. Having determined the five parameters at $\sqrt{s}=53$ GeV using the differential cross section and the total cross section data we inferred the values of the corresponding parameters at other energies using the concept of geometric scaling. Having determined the profile function we then studied the multiplicity distribution in pp collisions after the fashion of Ref. 20. Assuming Eq. (14) for the form of the KNO scaling function $\psi(z)$ we solved for the "up" and "down" solutions for the average multiplicity at a given impact parameter. These solutions are summarized in Eqs. (17) and (18). We tested some other proposals for the multiplicity distribution that have been made in the past and found that none of them give a satisfactory fit to the reduced moments when used in conjunction with our opacity.

ACKNOWLEDGMENT

We wish to acknowledge the help of Bob Teshima who wrote a very efficient program for the Bessel transform involved in Eq. (4).

---

*Work supported in part by the National Research Council of Canada.

[1]S. Fernbach, R. Serber, and T. B. Taylor, Phys. Rev. 75, 1352 (1949).
[2]T. T. Chou and C. N. Yang, Phys. Rev. 170, 1591 (1968); L. Durand III and R. G. Lipes, Phys. Rev. Lett. 20, 637 (1968).
[3]M. Elitzur and R. G. Lipes, Phys. Rev. D 7, 1420 (1973).
[4]F. Hayot and U. P. Sukhatme, Phys. Rev. D 10, 2183 (1974).
[5]V. Barger, in *Proceedings of the XVII International Conference on High Energy Physics, London, 1974,* edited by J. R. Smith (Rutherford Laboratory, Chilton, Didcot, Berkshire, England, 1974), p. I-193.
[6]J. Dias de Deus, Nucl. Phys. B59, 231 (1973); Nuovo Cimento Lett. 8, 476 (1973).
[7]A. J. Buras and J. Dias de Deus, Nucl. Phys. B71, 481 (1974).
[8]Z. Koba, H. B. Nielsen, and P. Olesen, Nucl. Phys. B40, 317 (1972).
[9]A. J. Buras and Z. Koba, Nuovo Cimento Lett. 6, 629 (1973).
[10]H. B. Nielsen and P. Olesen, Phys. Lett. 43B, 37 (1973).
[11]M. Le Bellac, J. L. Munier, and G. Plaut, Nucl. Phys. B62, 350 (1973).
[12]H. Moreno, Phys. Rev. D 8, 268 (1973).
[13]S. Barshay, Phys. Lett. 42B, 457 (1972).
[14]G. Auberson, T. Kinoshita, and A. Martin, Phys. Rev. D 3, 3185 (1971).
[15]U. Amaldi, Phys. (Paris) 34, 1 (1973).
[16]S. R. Amendolia *et al.*, Phys. Lett. 44B, 119 (1973).
[17]U. Amaldi *et al.*, Phys. Lett. 44B, 112 (1973).
[18]This point has been noted previously. See, for example, H. I. Miettinen, in *Proceedings of the Ninth Rencontre de Moriond,* edited by J. Tran Thanh Van (Université de Paris-Sud, Orsay, France, 1974), Vol. I, p. 363; F. S. Henyey, R. H. Tuan, and G. L. Kane, Nucl. Phys. B70, 455 (1974); R. Henzi and P. Valin, Phys. Lett. 48B, 119 (1974).
[19]G. Barbiellini *et al.*, Phys. Lett. 39B, 663 (1972).
[20]A. Białas and E. Białas, Acta Phys. Pol. B5, 373 (1974).
[21]P. Slattery, Phys. Rev. D 7, 2073 (1973).
[22]J. Whitmore [Phys. Rep. 10C, 273 (1974)] has given a review of the experimental situation (see pp. 296–297 of this reference).
[23]H. I. Miettinen, CERN Report No. Ref. TH.106-CERN, 1974 (unpublished).
[24]S.-J. Chang and T.-M. Yan, Phys. Rev. Lett. 25, 1586 (1970); Phys. Rev. D 4, 537 (1971); H. Cheng and T. T. Wu, Phys. Lett. 54B, 367 (1973).
[25]L. Caneschi and A. Schwimmer, Nucl. Phys. B44, 31 (1972); R. Aviv, R. L. Sugar, and R. Blankenbecler, Phys. Rev. D 5, 3252 (1972).
[26]*Handbook of Mathematical Functions,* edited by M. Abramowitz and I. A. Stegun, National Bureau of Standards Applied Mathematics Series, No. 55 (U.S.G. P.O., Washington, D. C., 1964), p. 824.